Community management indicators can conflate divergent phenomena: two challenges and a decomposition-based solution
Supporting Information

Georgina L Adams, Simon Jennings, Daniel C Reuman

Appendix S1: Proof of LFI slope decomposition

The slope of an ordinary linear regression can be calculated and decomposed as

$$slope = \frac{\sum x_i y_i - \frac{1}{n}\sum x_i \sum y_i}{\sum x_i^2 - \frac{1}{n}(\sum x_i)^2} = \frac{\sum_j^N \sum_i^n x_i y_{ij} - \frac{1}{n}\sum x_i \sum_j^N \sum_i^n y_{ij}}{\sum x_i^2 - \frac{1}{n}(\sum x_i)^2} = \sum_j^N \frac{\sum x_i y_{ij} - \frac{1}{n}\sum x_i \sum y_{ij}}{\sum x_i^2 - \frac{1}{n}(\sum x_i)^2}$$

where x_i is the explanatory variable (year), y_i is the dependent variable (LFI value), and n is the number of observations. If N is the number of components contributing to y_i, and y_{ij} is the LFI value for component j, then the slope is decomposed to the sum of the slopes for each component, j.

Appendix S2: Resampling method description

IBTS data were downloaded from the International Council for the Exploration of the Sea (ICES) Database of Trawl Surveys (DATRAS; datras.ices.dk) on 8 October 2013 for Q1 and 13 February 2014 for Q3. The specific structure of the IBTS data is important to the resampling method.

Firstly, the survey is stratified by ICES rectangle (1° x 0.5° grid cell). The survey design aims to carry out at least two hauls in each rectangle per year, so that catch rates can be averaged to give a mean catch rate per rectangle. In reality, the number of valid hauls per rectangle varies by year depending on factors such as weather conditions or the time or duration of hauls. An appropriate resampling method must respect this spatial structure of sampling by resampling within each haul, not within or across rectangles.

Secondly, each row/entry of the IBTS data comprises the number of individuals caught in a length category of a species in a haul. In order for the resampling method to approximate repeated survey efforts, it should resample on this unit, i.e. on the actual number of fish caught by species-length category within a haul. This requires being able to resample from the raw number of individuals caught. However, this is complicated by fact that the IBTS data on DATRAS includes scaled up numbers rather than raw catch numbers when large catches are subsampled (Table S1, row 2). Subsampling is used because large numbers of individuals of abundant species may be caught in individual hauls, so every individual cannot be counted or measured. Subsampling factors are either reported or can be calculated from the data, and these are needed to transform recorded catch rates back into raw catch numbers per species-length category, in the cases where raw catch numbers were not directly presented in the data. For some rows in the database, reported subsampling factors were incorrectly recorded or absent, so corrected estimates of actual numbers of fish measured per length category were obtained by calculating the corrected subsampling factor as the total catch column divided by the number of individuals measured (Table S1). The corrected subfactor (Table S1) is then used to generate a corrected catch at length (catch at length (true) in Table S1). Taking any subsampling factors into account is important for the resampling procedure, as this process of scaling up catch numbers based on subsamples will result in sampling variation being greatly inflated for large catches.

We developed a resampling method to reproduce the true levels of sampling variation in the data. The method used parametric bootstrapping to generate surrogate IBTS data sets. The surrogate data sets were intended to represent repeated sampling as closely as possible, that is, as if the IBTS survey were carried out in the North Sea multiple times, retaining spatial structure in the survey design. Resampling in this way means that surrogate data can be used in the same way as the original data. Thus any metric or trend calculated from the original data can also be calculated with the surrogate data, providing a distribution of values from which confidence intervals can be calculated.

Resampling was carried out as follows. For each haul in each location and year, the true number of individuals caught in each species-length category was calculated using either the recorded or corrected subsampling factor (in cases where no subsampling occurred and every individual caught was measured, a subsampling factor of 1 was used). This is the value in the column "catch at length (true)" in Table S1. True catch number was used as the resampling unit. This is essential to ensure that sampling variation in the catch numbers is correctly estimated before being scaled up by the subsampling factor. This, in turn, ensures that variation is amplified in the resampled data in the same way as in the real data.

A parametric-bootstrapped dataset was then generated by drawing values from a Poisson distribution, where the Poisson parameter was taken as the true catch-at-length. This method of resampling makes some assumptions/ idealisations about the data. First, it assumes that the sampling variability in the data, given trawl stations fixed in space and time, was principally due to by-chance catching of different numbers of individuals in any given haul. Second, it assumes that the number of individuals

2

caught in any species-length category can be described by a Poisson distribution. Finally, it assumes that resampling can be carried out independently for different species-length categories and different hauls. These idealisations are revisited in Appendix S3.

The resampled catch-at-length numbers were used to produce surrogate IBTS data sets. Resampled catch-at-length values were generated 1000 times for each species-length category in each haul (i.e. for each row of the IBTS data set). Resampled values were then multiplied by the corrected subsampling factor where required, and converted into a catch rate (catch per unit effort; cpue) averaged by haul duration (usually 30 minutes). Surrogate data sets were then "cleaned" in the same way as the IBTS data itself (details of data "cleaning" follow in Section S4). This resulted in 1000 surrogate datasets with the same spatial and temporal sampling distribution as the original IBTS data, with catch numbers drawn from the same species-length distribution as in the original data, but including an estimate of sampling variation at the level of species and length classes.

For each indicator (e.g., the LFI) calculated from the resampled data, confidence intervals were estimated by calculating the metric for each surrogate dataset, and then taking percentiles from the resulting distribution of values. By resampling the data in this way, rather than using a bootstrapping method that resamples at the level of entire hauls (e.g. the method used by Shephard *et al.* 2012 for the LFI in the Celtic Sea), the spatial structure of the IBTS survey is preserved. This allows appropriate confidence intervals to be assigned to components of spatial decompositions. Confidence intervals were 95% for all analyses.

Appendix S3: Assumptions and limitations of the methods

The parametric bootstrap method we developed for the IBTS resamples catch rates from a Poisson distribution. A Poisson distribution was chosen because it is a discrete distribution that takes non-negative integer values, and the number of fish caught in each species-length category (the unit we resampled from) is a non-negative integer. The resampling method assumes that the number of individuals caught in any species-length category can be described by a Poisson distribution. However, fish behaviour may influence catch numbers in each species-length category in at least two ways, making a Poisson distribution an approximation. Firstly, the schooling behaviour of fish in some species makes it more likely that fish will either be caught in large numbers or not at all, and the Poisson distribution may not adequately reflect this. Secondly, the presence/absence of individuals in the trawl path may influence the presence/absence of individuals in a different species or size category, invalidating the assumption of independence of resampling among rows of the database. For example, if a higher number of large predators are present in a trawl path, we might expect that the numbers of smaller prey fish will be correspondingly lower. To resample while accounting for these and other behavioural traits would require a much more complex scheme. Our view is, such a scheme would require so many assumptions about the nature of fish behaviour and population dynamics as to render it inaccurate and minimally useful. Our simpler, approximate approach is more appropriate.

The resampling methods we developed and applied can be adapted to a wide variety of community indicators other than the LFI, but probably cannot be applied to diversity-based indicators. The Poisson distribution used in resampling allows a value of zero for individuals caught in a species-length category, but this is vanishingly unlikely except in low-abundance categories. In these rare cases species richness in a resampled dataset would decrease if rare species are resampled as being caught zero times. Furthermore, species richness cannot increase, since our resampling scheme cannot create new species-length categories. Thus, at sea, it is critical that the whole catch should be sorted for all species present before any of the more abundant species are sub-sampled. Nevertheless, our resampling approach should apply to indicators not based on diversity, and the insights gained from applying our approach to the LFI suggests adapting it to other indicators would be worthwhile.

Appendix S4: Cleaning the IBTS data

IBTS data were cleaned following Daan (2001), Fung *et al*. (2012), and the IBTS survey manual (ICES 2012), with some updated adjustments and modifications. Hauls taken at night, or with a duration of less than 15 minutes were removed (ICES 2012; Petrakis 2001). Species names were assigned from the WoRMS (World Register of Marine Species; www.marinespecies.org) and ITIS (Integrated Taxonomic Integration System; www.itis.gov) databases using the R package taxize (Chamberlain and Szocs, 2013); individuals in the survey are identified to species level where possible, and genus, family or occasionally order where not. All non-fish species (shellfish, cephalopods) were removed from the dataset. To ensure consistency across all vessels, lengths were standardised to 1cm intervals for all fish species except herring and sprat (which were standardised to 5mm categories). Individual records where incorrect lengths had been recorded were removed in the following way: any individual that was recorded as being over 10% longer than the maximum length recorded for its species (obtained from a list of North Sea maximum lengths by species on FishBase (www.fishbase.org) on 12/12/2013) was discarded from the data. Length categories were converted to mass using species-specific length-mass regressions where possible (Table S2; ICES 2014) from Silva *et al.* (2013), and the standard regression coefficients of 0.01 and 3 for fish elsewhere (Table S2; Blanchard *et al.*, 2005; ICES, 2014). Some indicators and studies suggest that pelagic species should be removed (Greenstreet *et al.* 2011; Shephard *et al.* 2011) as they don't form part of the demersal community that is sampled by the standard GOV trawl gear used for the IBTS. However, they are an important part of the North Sea fish community and several very abundant and important small species (sprat, herring) are considered to be pelagic. These species were left in for the main analyses but alternative analyses with pelagic species removed were carried out for comparison.

Catch rate per unit effort (cpue; unit effort is one hour) was then calculated for each length category per species per haul; hauls are typically 30 minutes in duration but there is some variation in the data. Catch rate per unit area (cpua; unit area is per m^2) was calculated following Fraser *et al.* (2007) to obtain catch rates that were corrected for the area swept by the gear in each haul. Catch rates were then averaged over hauls in each ICES rectangle. To make the data comparable temporally and spatially, ICES rectangles were grouped into 1x1 degree grid cells, and any grid cell with missing hauls in more than 2 years was discarded entirely (Greenstreet *et al.* 2012). The same grid cells were included in every year. Q1 data was restricted to the same grid cells as in Q3, because the Q3 survey is a more limited survey both spatially and temporally. The IBTS extends into areas that are typically defined as being outside of the North Sea region (Kattegat and Skaggerat) so ICES rectangles in these areas were removed from the data. LFI trends in our data were similar to those reported for other cleaning treatments of the data (Fig. S9).

Appendix S5: Decomposition of large fish biomass slopes

Large fish biomass vs LFI

For the main analyses, we decomposed the LFI slope into constituent parts. The LFI is a ratio (see Equation 1 in Methods in the main text), and thus changes in the LFI and its slope may have been due to changes in large fish biomass, small fish biomass, or both (Fig. 1 in main text). We therefore decomposed the large fish biomass slope (the numerator in the LFI) in additional analyses, which allowed us to interpret whether the numerator (large fish) or the denominator (both small and large fish) drove trends in the LFI. Since large fish biomass is a single additive metric, summands in its decomposition are simply the independently-computed values for that component, unlike for the LFI.

When changes in small fish biomass are greater than those in large fish biomass, component slopes in the LFI and in large fish biomass may disagree. For example, a species may have a positive contribution to the LFI slope, but a negative contribution in its large fish biomass. This was not common in our results but did occur. Comparisons between LFI slope contributions and large fish biomass slope contributions are discussed below.

Species decomposition

Most species that made up a substantial component of the LFI slope showed a similar contribution (in both magnitude and sign) to the large fish biomass slope, but among the dominant contributors there were a few notable exceptions. Saithe *Pollachius virens* was the largest contributor to the LFI slope in both Q1 and Q3 (Fig. 2 in main text), and its large fish biomass slope was also the largest positive contributor in Q1 (Fig. S3). However, in Q3, it has a smaller, non-significant large fish biomass contribution. Another exception was haddock *Melanogrammus aeglefinus* which had a large, positive contribution to the LFI slope in both quarters, but the large haddock biomass slope only mirrored this in Q3: the large haddock biomass slope was negative in Q1 (Fig. S3). A positive haddock contribution to the Q1 LFI slope was possible in spite of a negative haddock contribution to Q1 large fish biomass slope because the overall negative Q1 change in total fish biomass was stronger than the negative Q1 change in large haddock biomass.

Spatial decomposition

The patterns of LFI contributions across grid cells (Fig. 3 in main text) were generally consistent with patterns of change in total large fish biomass (Fig. S4), with a few exceptions. The grid cells with the most dominant contributions all showed agreement between their LFI slope and large fish biomass slope contributions, across both Q1 and Q3. However, there were a number of less dominant grid cells where a negative large fish biomass slope contribution produced a positive LFI slope contribution. In the north North Sea where most grid cells showed consistency in LFI and large fish biomass slope contributions, grid cell 1x60 was an exception, being a positive contributor to the LFI slope in Q1 and in Q3, but a negative contributor to the large fish biomass slope in both quarters. In the central and southern regions, where LFI slope contributions tended to be smaller, there was less consistency with large fish biomass slopes.

Appendix S6: Alternative analyses

The large fish indicator is usually calculated using catch per unit area (cpua) as the measure of abundance. This was adopted for the analysis presented in the main text, but we also repeated the analysis using catch per unit effort (cpue). Catchability corrections for most species (Fraser *et al.*, 2007) were applied to both cpua and cpue for comparison in additional alternative analyses, but were not used in the analysis presented in the main text because they are not available for all species and are not completely independent of the trawl data. A large fish cut off of 40cm was used, as is defined for the North Sea LFI, but alternative analyses also considered other cut-offs of 35cm and 45cm. The IBTS data are sometimes subsetted by removing pelagic species (as they are not part of the bottom dwelling community and are not so readily caught by the IBTS trawl gears) or by removing individuals under 20cm in length (which may be under-sampled by the IBTS trawl or may be more sensitive to changes in phenology) before calculating LFI denominators. Both sets of restrictions were included in alternative analyses, but not adopted in the main analysis.

The main conclusions drawn from the results of the analysis presented in the accompanying paper were robust to these alternative analyses. In all alternative analyses, both species and spatial LFI decompositions showed heterogeneity in the magnitude and sign of the component trends. This was the case for both Q1 and Q3 LFI trends. Further, in all alternative analyses, only a few species and grid cells determined the overall LFI trend, as in the main analysis. The abundant and commercially important species that were large contributors to the LFI trend in the main analysis (*Pollachius virens* (saithe), *Gadus morhua* (cod), *Melanogrammus aeglefinus* (haddock), M*erlangius merlangus* (whiting) and *Merluccius merluccius* (hake)) were also large contributors in all alternative analyses, for both quarters. The contributions of each of these important species had the same sign in the alternative analyses as in the main analysis, with the exception of haddock in Q1 which switched from a positive to a negative contribution when a large fish cut-off of 45cm was used.

Supplementary references

Blanchard, J., Dulvy, N., Jennings, S., Ellis, J., Pinnegar, J., Tidd, A., Kell, L. (2005) Do climate and fishing influence size-based indicators of Celtic Sea fish community structure? *ICES Journal of Marine Science*, **62**, 405–411.

Chamberlain, S.A. & Szöcs, E. (2013) taxize: taxonomic search and retrieval in R. *F1000Research* 2013, 2:191 (doi: 10.12688/f1000research.2-191.v2)

Daan, N. (2001) The IBTS database: a plea for quality control. ICES Document CM 2001/T: 03. 19 pp.

Fraser, H.M., Greenstreet, S.P.R. & Piet, G.J. (2007) Taking account of catchability in groundfish survey trawls: implications for estimating demersal fish biomass. *ICES Journal of Marine Science*, **64**, 1800–1819.

Fung, T., Farnsworth, K.D., Reid, D.G., Rossberg, A.G. (2012) Recent data suggest no further recovery in North Sea Large Fish Indicator. *ICES Journal of Marine Science*, **69**, 235–239.

Greenstreet, S.P.R., Rogers, S.I., Rice, J.C., Piet, G.J., Guirey, E.J., Fraser, H.M., Fryer, R.J. (2011) Development of the EcoQO for the North Sea fish community. *ICES Journal of Marine Science*, **68**, 1–11.

Greenstreet, S.P.R, Fraser, H.M., Rogers, S.I., Trenkel, V.M., Simpson, S.D., Pinnegar, J.K. (2012) Redundancy in metrics describing the composition, structure, and functioning of the North Sea demersal fish community. *ICES Journal of Marine Science*, **69**, 8–22.

ICES (2012) *Manual for the International Bottom Trawl Surveys.* Series of ICES Survey Protocols. SISP 1-IBTS VIII. 68 pp.

ICES (2014) *Report of the Working Group on the Ecosystem Effects of Fishing Activities (WGECO)*. Copenhagen, Denmark.

Petrakis, G. (2001) Day–night and depth effects on catch rates during trawl surveys in the North Sea. *ICES Journal of Marine Science*, **58**, 50–60.

Shephard, S., Reid, D.G., Greenstreet, S.P.R. (2011) Interpreting the large fish indicator for the Celtic Sea. *ICES Journal of Marine Science*, **68**, 1963–1972.

Shephard, S., Fung, T., Houle, J.E., Farnsworth, K.D., Reid, D.G., Rossberg, A.G. (2012) Size-selective fishing drives species composition in the Celtic Sea. *ICES Journal of Marine Science*, **69**, 223–234.

Silva, J.F., Ellis, J.R., Ayers, R.A. (2013) Length-weight relationships of marine fish collected from around the British Isles. *Sci. Ser. Tech. Rep. Cefas Lowestoft*, **150**, 109pp.
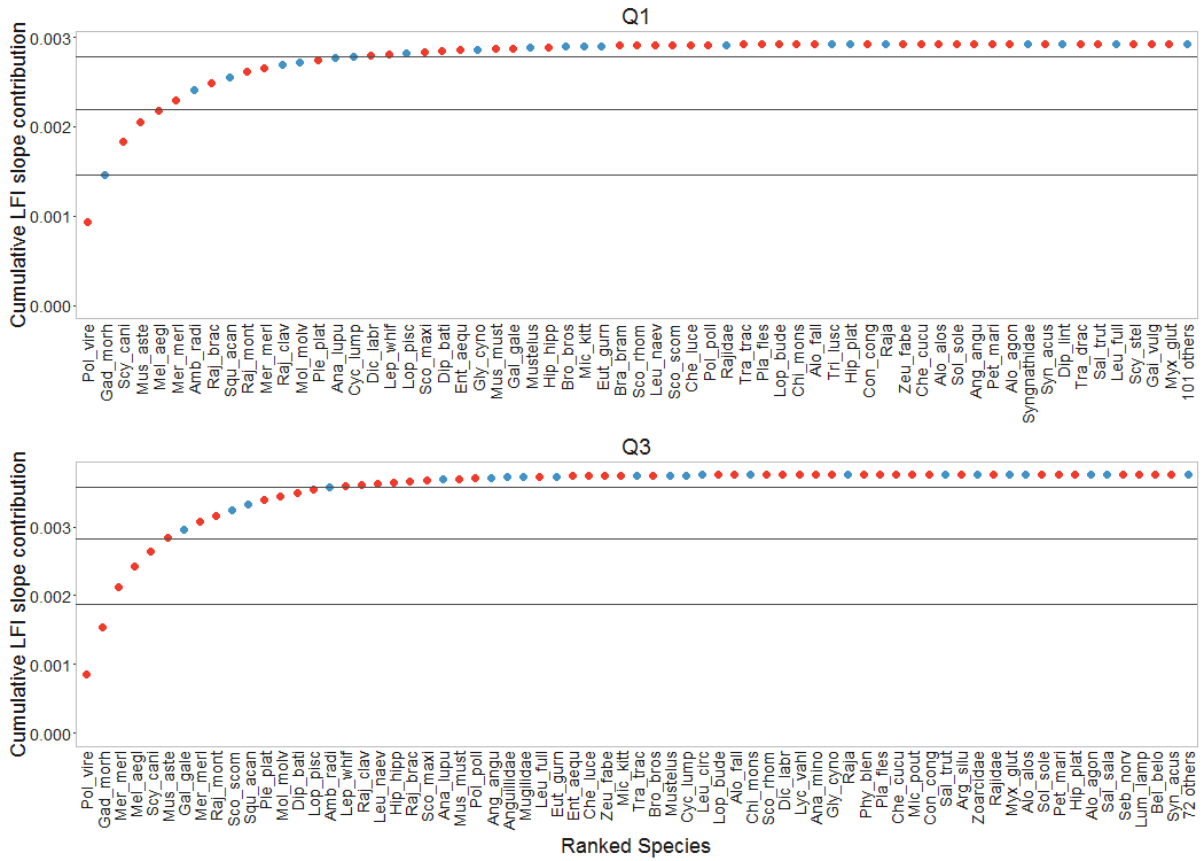
Figure S1: Ranked contributions to the slope of the LFI, decomposed by species. Values are on a linear scale, and are absolute values of the slope contribution for each species, ranked in size from largest to smallest. Red points represent a positive contribution, blue a negative one. Horizontal lines show 50%, 75% and 95% of the sum of the absolute values of all contributions. Species names are truncated, a list of species and their truncated names is provided in Table S2.
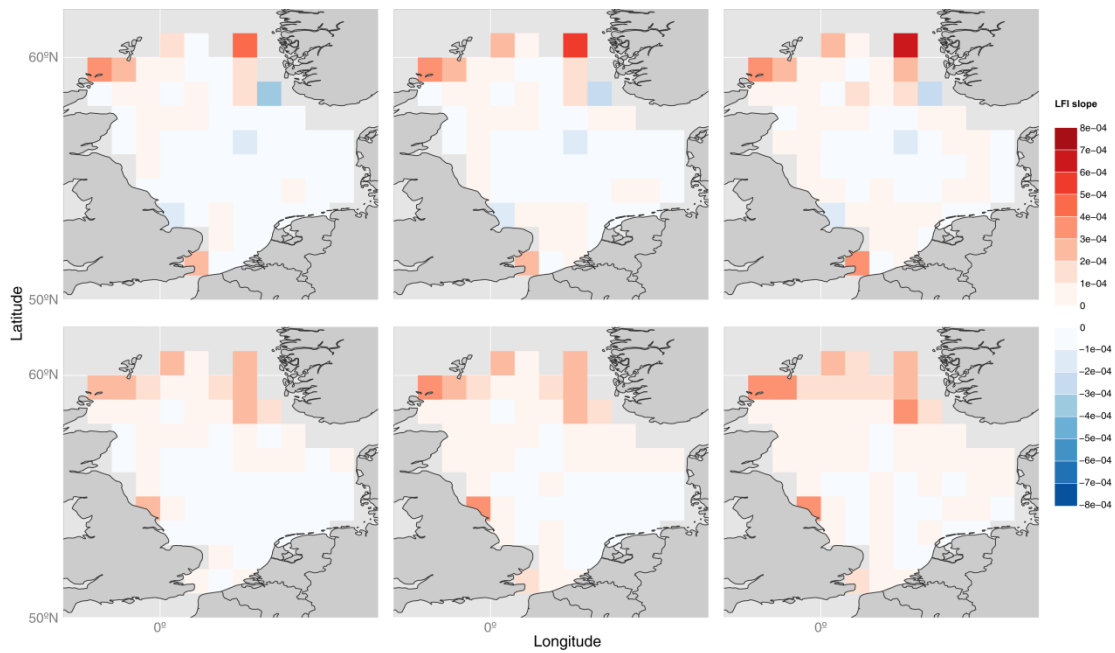
Figure S2: Decomposition of the LFI slope by 1°x1° grid cells. This is analogous to Figure 3 in the accompanying paper, but the colours are now on a linear scale to highlight differences in the magnitudes of contributions across grid cells.

Figure S3: Decomposition of the total large fish biomass slope by species. Analogous to Figure 2 in the accompanying paper, but calculated using large fish (> 40cm in length) biomass totals for each species rather than the LFI.
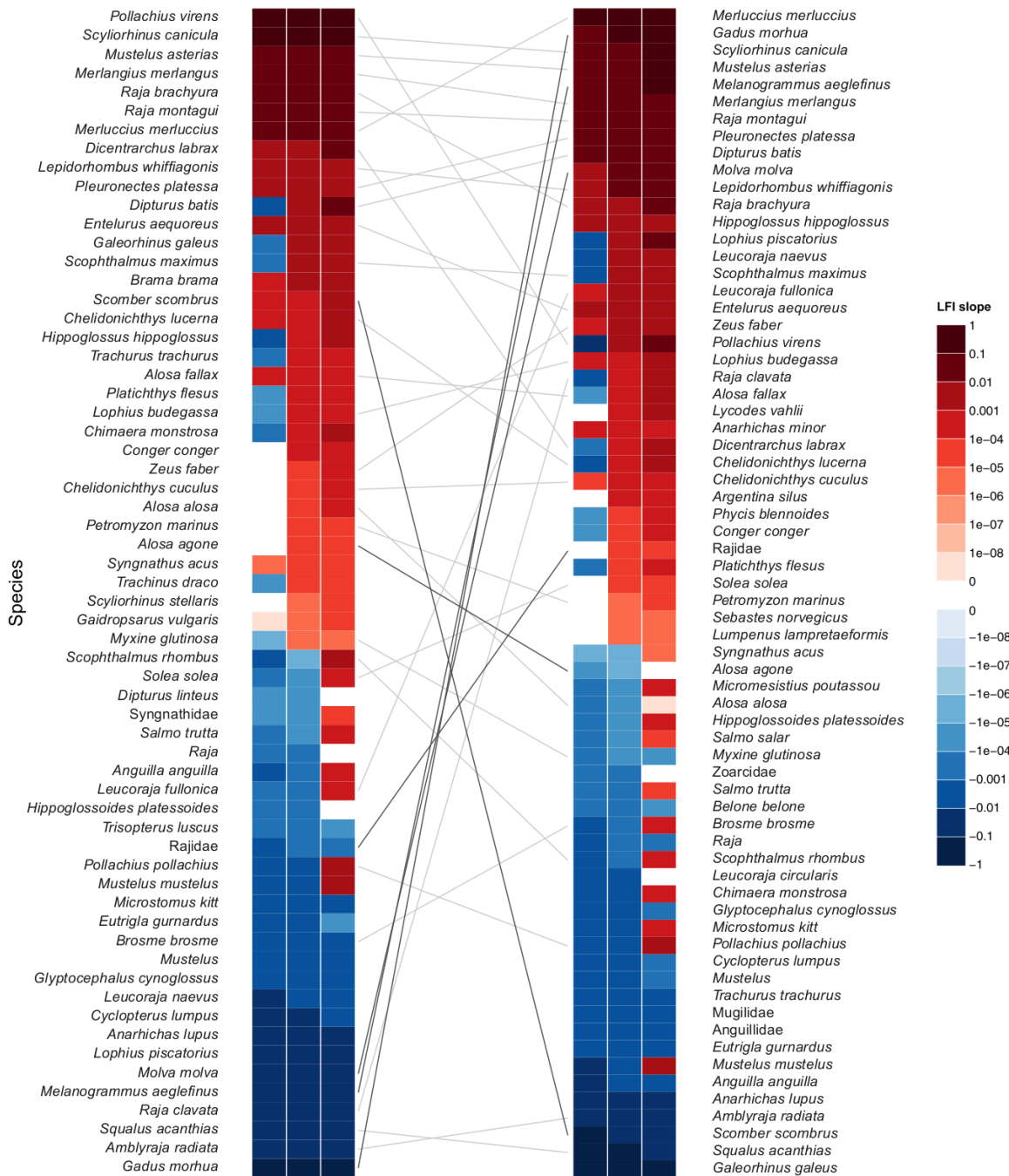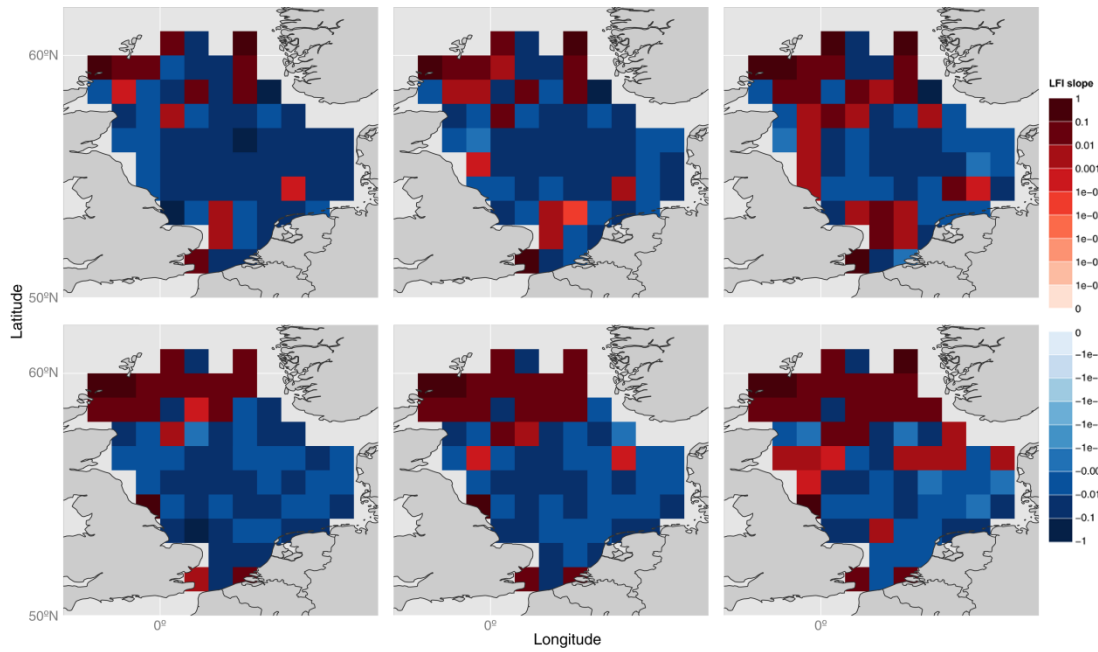
Figure S4: Decomposition of the total large fish biomass slope by 1°x1° grid cell. This is analogous to Figure 3 in the accompanying paper but calculated using large fish (> 40cm in length) biomass rather than the LFI.
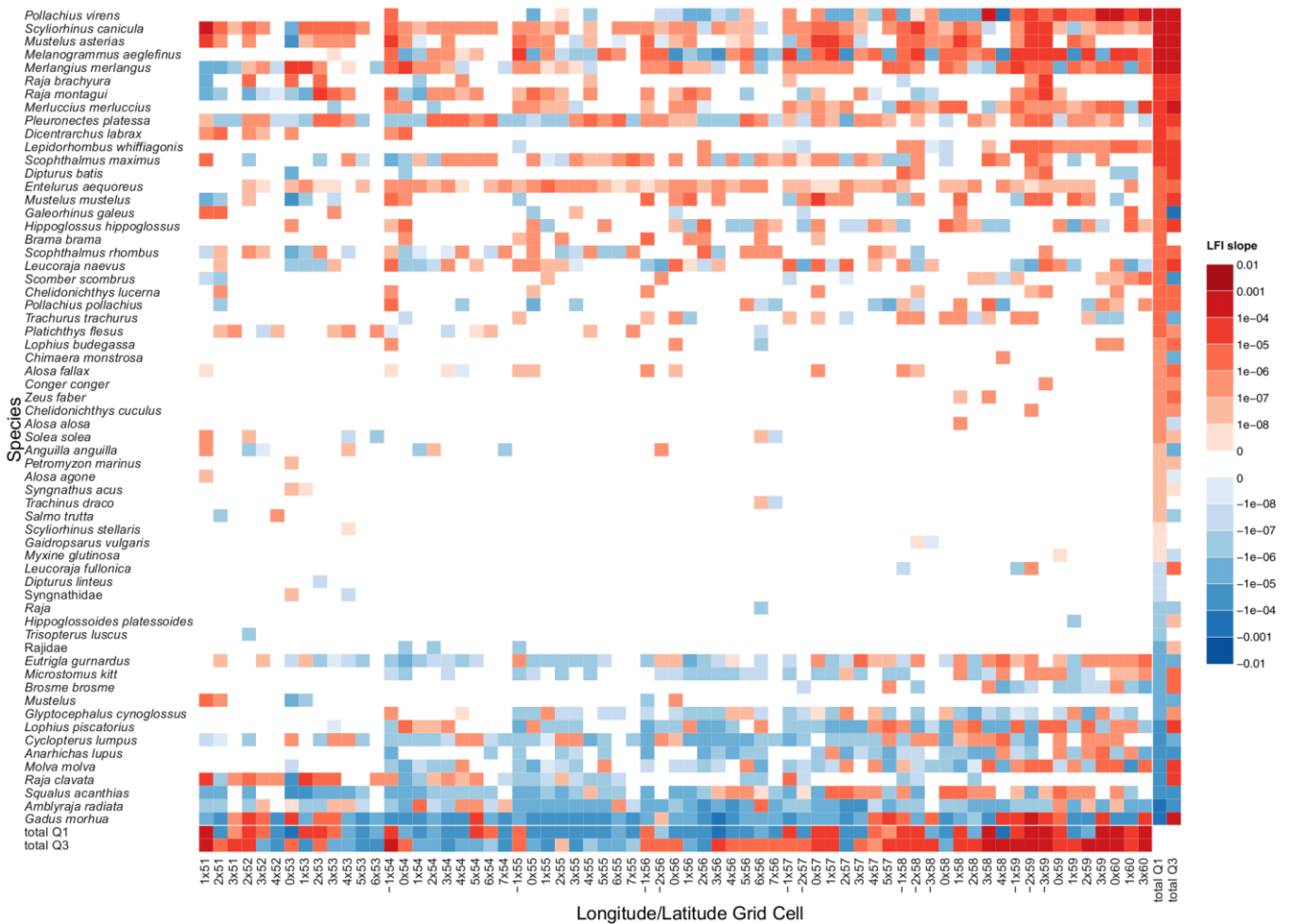
Figure S5: Heat map showing the decomposition of the LFI slope by both species and by 1°x1° grid cell, for Q1. Values are represented on a log scale, red represents a positive contribution to the overall slope and blue a negative contribution. Species are ordered on the y-axis by magnitude of total contribution. Grid cells are ordered on the x-axis from lower latitude bands to higher latitude bands. Total columns show the sum of contributions across all grid cells for each species, the first total column is for the quarter represented by the plot, the second for the species total in the opposite quarter to enable comparison (if a species has a contribution in both quarters). These species totals are the same as in Figure 2 in the accompanying paper. Total rows show the sum of contributions across all species for each grid cell, the first column is for the quarter represented by the plot, the second for the grid cell total in the opposite quarter to enable comparison. These totals for each grid cell are the same as in Figure 3 in the accompanying paper.

Figure S6: Heat map showing the decomposition of the LFI slope by both species and by 1°x1° grid cell, for Q3. Values are represented on a log scale, red represents a positive contribution to the overall slope and blue a negative contribution. Species are ordered on the y-axis by magnitude of total contribution. Grid cells are ordered on the x-axis from lower latitude bands to higher latitude bands. Total columns show the sum of contributions across all grid cells for each species, the first total column is for the quarter represented by the plot, the second for the species total in the opposite quarter to enable comparison (if a species has a contribution in both quarters). These species totals are the same as in Figure 2 in the accompanying paper. Total rows show the sum of contributions across all species for each grid cell, the first column is for the quarter represented by the plot, the second for the grid cell total in the opposite quarter to enable comparison. These totals for each grid cell are the same as in Figure 3 in the accompanying paper
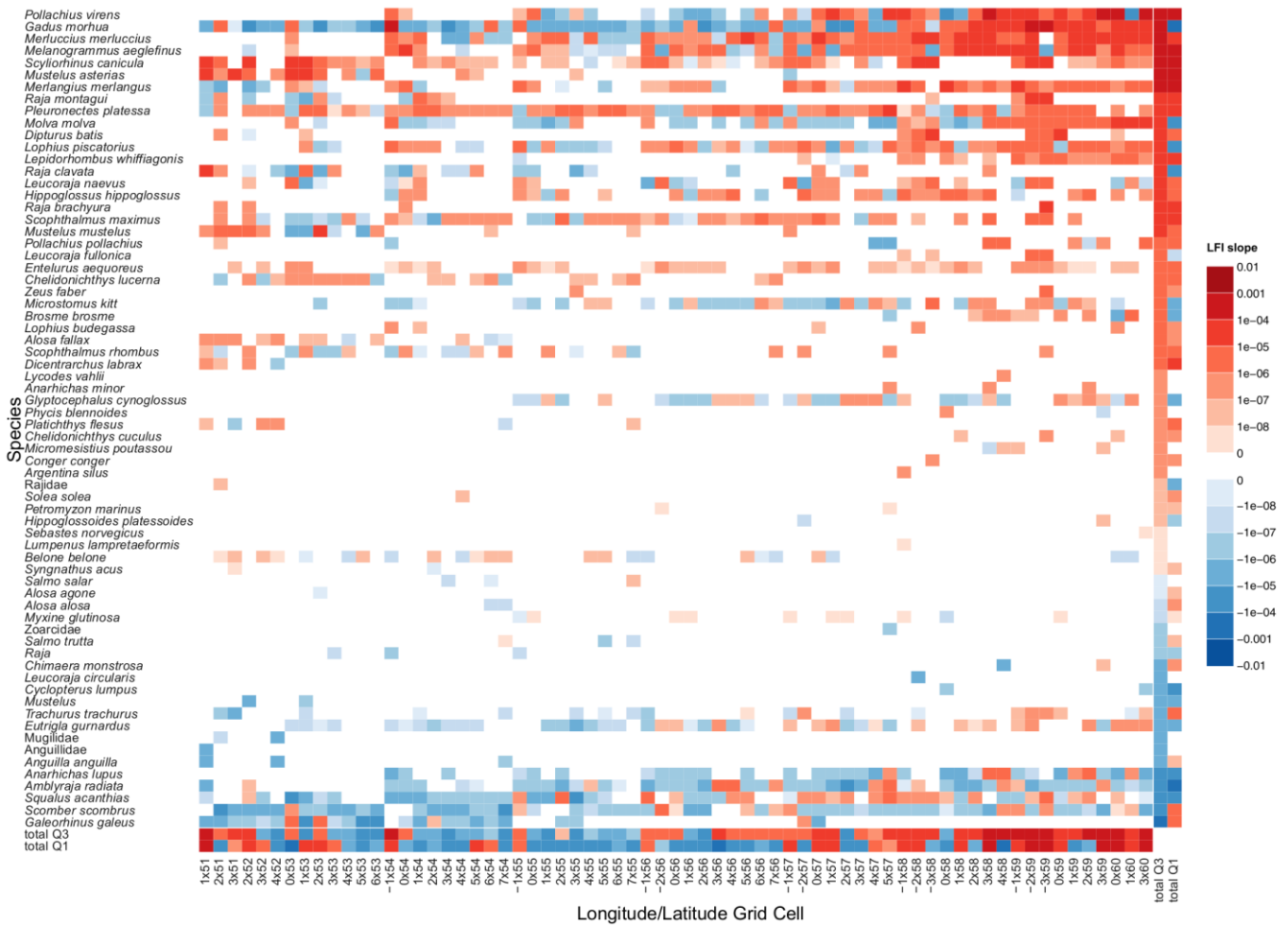
14

Figure S7: Contributions to the LFI slope, decomposed by 1°x1° grid cell in Q1, for each of five species that are abundant and make a large contribution to the LFI slope (*Pollachius virens* (saithe), *Gadus morhua* (cod), *Melanogrammus aeglefinus* (haddock), *Merlangius merlangus* (whiting) and *Merluccius merluccius* (hake)). The middle column in each row is the point estimate, the left column is the lower 95% confidence interval bound based on 1000 resampled datasets, and the right column is the upper 95% confidence interval bound. Values are represented on a log scale, red represents a positive contribution to the overall slope and blue a negative contribution. White cells represent a contribution of zero to the overall slope, where surveys were carried out but no large fish from that particular species were found. Figure 5 in the accompanying paper shows the middle column of panels only.
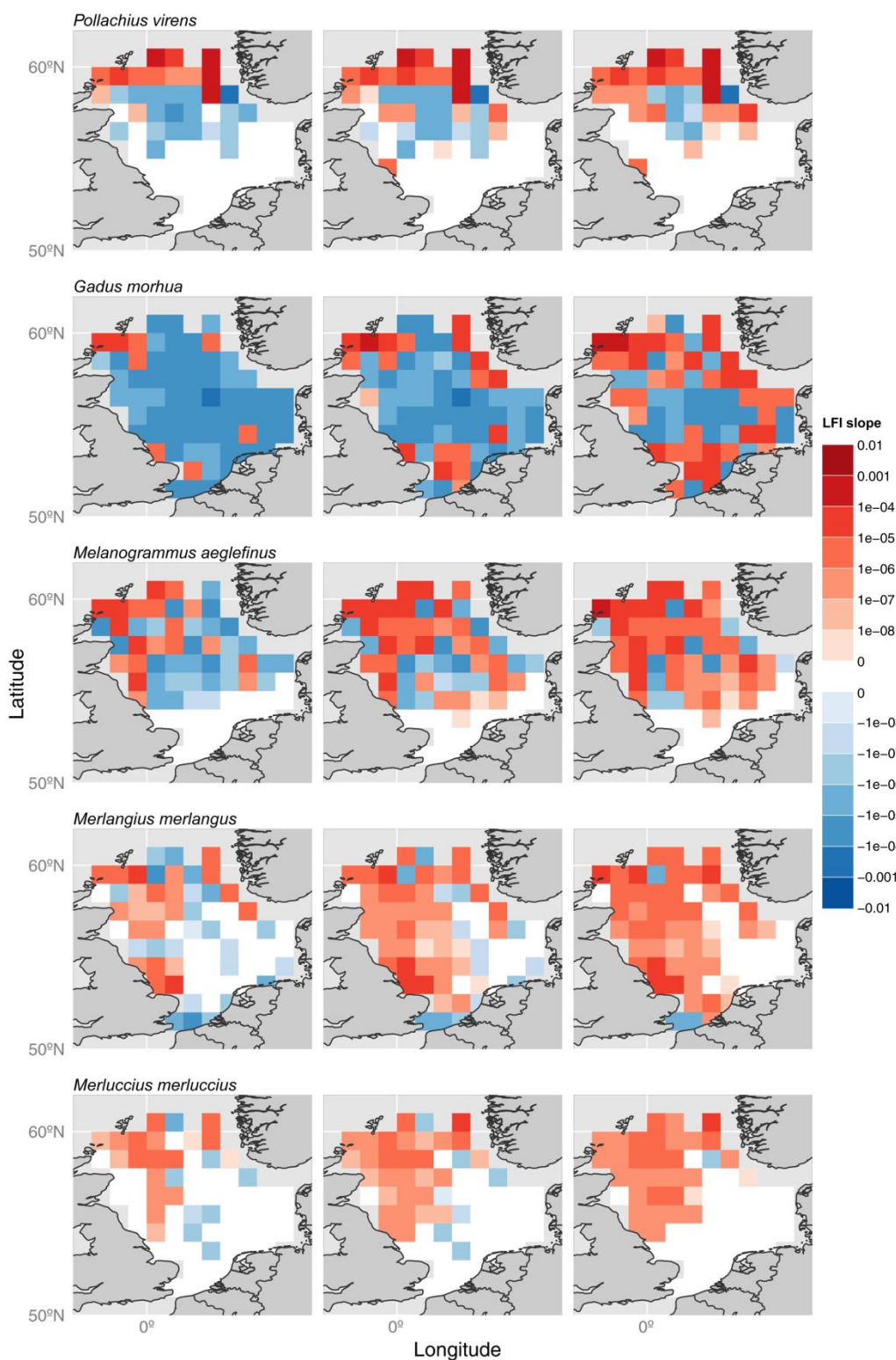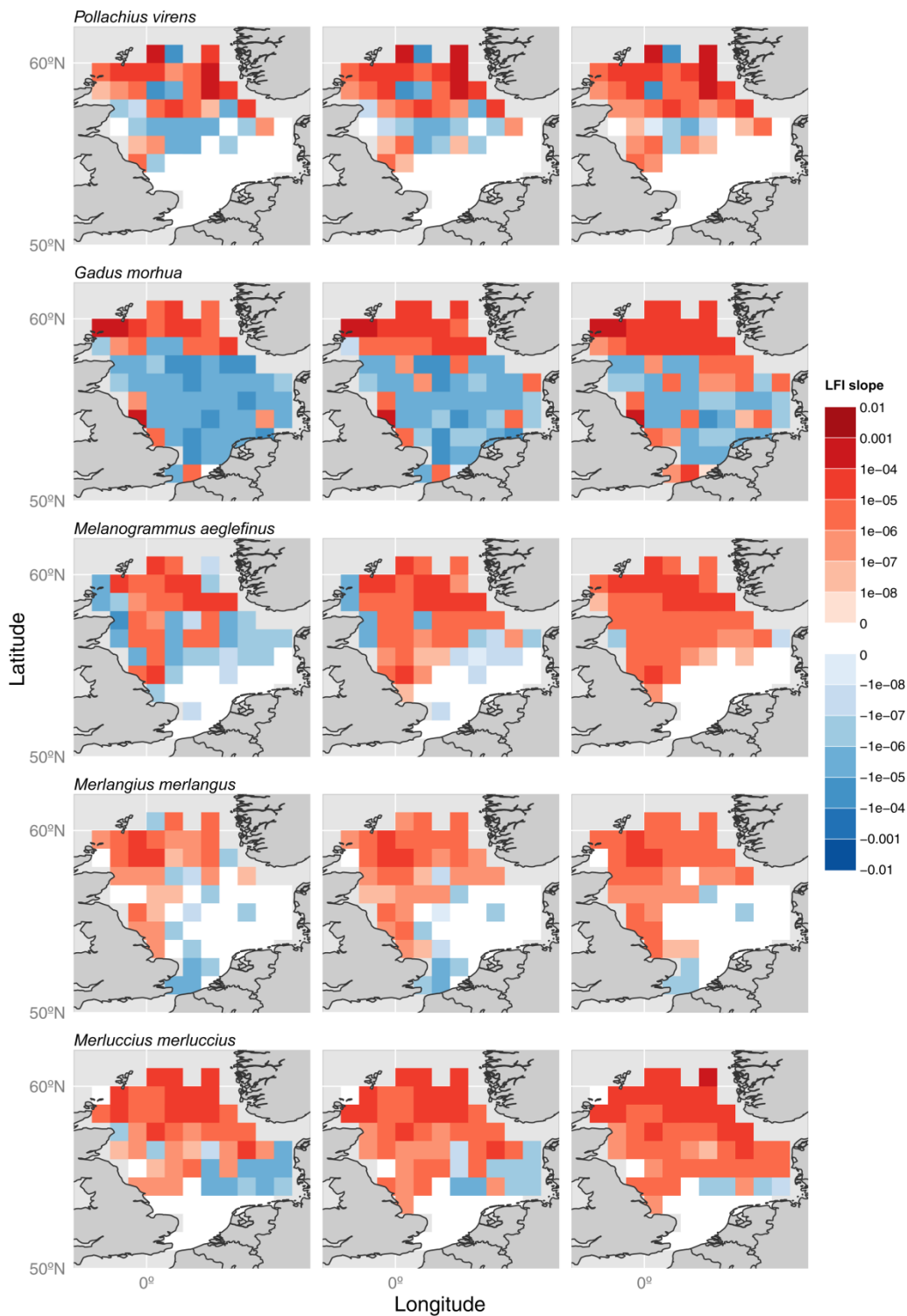
Figure S8: Contributions to the LFI slope, decomposed by 1°x1° grid cell in Q3, for each of five species that are abundant and make a large contribution to the LFI slope (*Pollachius virens* (saithe), *Gadus morhua* (cod), *Melanogrammus aeglefinus* (haddock), *Merlangius merlangus* (whiting) and *Merluccius merluccius* (hake)). The middle column in each row is the point estimate, the left column is the lower 95% confidence interval bound based on 1000 resampled datasets, and the right column is the upper 95% confidence interval bound. Values are represented on a log scale, red represents a positive contribution to the overall slope and blue a negative contribution. White cells represent a contribution of zero to the overall slope, where surveys were carried out but no large fish from that particular species were found.

16

Figure S9: LFI values between 1991 and 2013 for Q1 IBTS data, as calculated for the main analysis using the cleaning methods detailed in Appendix S3 (solid line), and as calculated for an alternative analysis (Appendix S6) excluding pelagic species and length categories under 20cm (dash-dotted line), together with Q1 LFI values taken from two previously published studies of the LFI in the North Sea (Greenstreet *et al.* 2011 (dotted line) and Fung *et al.* 2012 (dashed line)). LFI trends calculated using data cleaned for our main analysis are similar to previously reported trends, but LFI values are lower overall, due to the inclusion of smaller individuals and pelagic species in the LFI denominator.

Table S1: Example rows of the IBTS data, taken from the Q1 survey data.

Species	Total catch	No. individuals measured	Subfactor (reported)	Length class (cm)	Catch at length (recorded)	Subfactor (corrected)	Catch at length (true)	cpue
Limanda limanda	15	15	1	14	2	1	2	4
Merlangius merlangus	178	89	1	15	50	2	25	100

Table S2: Species included in the analysis of the IBTS survey data, with truncated species names as used in some plots. In some cases, the data included only identification to genus level or higher; genus and family names listed here may represent one or more species in that category. Species-specific mass-length regression coefficients from Silva *et al*. (2013) are listed as *a* and *b*, used in the form $W=aL^b$, where W is mass (g) and L is length (cm). Values of 0.01 and 3 were used where no species-specific coefficients were available. The final column indicates which survey the species was present in, Q1, Q3 or both.

Species	Truncated species name	*a*	*b*	Pelagic (P) or demersal (D)	Quarter
Acentronura		0.01	3	D	Q1
Agonus cataphractus	Ago_cata	0.0232	2.5916	D	Q1, Q3
Alosa agone	Alo_agon	0.01	3	P	Q1, Q3
Alosa alosa	Alo_alos	0.00492	3.20165	P	Q1, Q3
Alosa fallax	Alo_fall	0.01	3	P	Q1, Q3
Amblyraja radiata	Amb_radi	0.0107	2.94	D	Q1, Q3
Ammodytes		0.01	3	D	Q1, Q3
Ammodytes marinus	Amm_mari	0.0017	3.1828	D	Q1, Q3
Ammodytes tobianus	Amm_tobi	0.01	3	D	Q1, Q3
Ammodytidae		0.01	3	D	Q1, Q3
Anarhichadidae		0.01	3	D	Q1
Anarhichas lupus	Ana_lupu	0.0046	3.1849	D	Q1, Q3
Anarhichas minor	Ana_mino	0.01	3	D	Q3
Anguilla anguilla	Ang_angu	0.01	3	D	Q1, Q3
Anguillidae		0.01	3	D	Q3
Aphia minuta	Aph_minu	0.01	3	P	Q1, Q3
Argentina		0.01	3	D	Q1, Q3
Argentina silus	Arg_silu	0.01	3	D	Q1, Q3
Argentina sphyraena	Arg_sphy	0.0053	3.0534	D	Q1, Q3
Arnoglossus		0.01	3	D	Q1
Arnoglossus imperialis	Arn_impe	0.007	3.0541	D	Q1, Q3
Arnoglossus laterna	Arn_late	0.0198	2.6673	D	Q1, Q3
Atherina presbyter	Ath_pres	0.01	3	P	Q1
Belone belone	Bel_belo	2.00E-04	3.442	P	Q1, Q3
Blenniidae		0.01	3	D	Q1
Bothidae		0.01	3	D	Q1
Brama brama	Bra_bram	0.01	3	P	Q1
Brosme brosme	Bro_bros	0.00514	3.189	D	Q1, Q3
Buglossidium		0.01	3	D	Q1
Buglossidium luteum	Bug_lute	0.0157	2.9092	D	Q1, Q3
Callionymidae		0.01	3	D	Q1, Q3
Callionymus		0.01	3	D	Q1
Callionymus lyra	Cal_lyra	0.021	2.647	D	Q1, Q3
Callionymus maculatus	Cal_macu	0.0369	2.2653	D	Q1, Q3
Callionymus reticulatus	Cal_reti	0.0296	2.3367	D	Q1, Q3
Capros aper	Cap_aper	0.0549	2.6322	D	Q1, Q3
Chelidonichthys cuculus	Che_cucu	0.0089	3.0257	D	Q1, Q3
Chelidonichthys lucerna	Che_luce	0.0106	2.9846	D	Q1, Q3
Chimaera monstrosa	Chi_mons	0.01	3	D	Q1, Q3
Ciliata mustella	Cil_must	0.01	3	D	Q1

Ciliata septentrionalis	Cil_sept	0.0092	2.9846	D	Q1, Q3
Clupea harengus	Clu_hare	0.0026	3.3687	P	Q1, Q3
Conger conger	Con_cong	2.00E-04	3.5789	D	Q1, Q3
Cottidae		0.01	3	D	Q1
Crystallogobius linearis	Cry_line	0.01	3	P	Q1, Q3
Ctenolabrus rupestris	Cte_rupe	0.015	3.0403	D	Q1, Q3
Cyclopteridae		0.01	3	D	Q1
Cyclopterus lumpus	Cyc_lump	0.0587	2.939	D	Q1, Q3
Dicentrarchus labrax	Dic_labr	0.0103	3.0047	D	Q1, Q3
Diplecogaster bimaculata	Dip_bima	0.0589	1.8205	D	Q1
Dipturus batis	Dip_bati	0.0038	3.1201	D	Q1, Q3
Dipturus linteus	Dip_lint	0.01	3	D	Q1
Echiichthys vipera	Ech_vipe	0.0186	2.8398	D	Q1, Q3
Echiodon drummondii	Ech_drum	0.01	3	D	Q1, Q3
Enchelyopus cimbrius	Enc_cimb	0.008	2.8377	D	Q1, Q3
Engraulis encrasicolus	Eng_encr	0.005	3.1072	P	Q1, Q3
Entelurus aequoreus	Ent_aequ	8.00E-04	2.5939	P	Q1, Q3
Eutrigla gurnardus	Eut_gurn	0.0091	2.9772	D	Q1, Q3
Gadiculus argenteus	Gad_arge	0.016	2.7931	D	Q1, Q3
Gadus morhua	Gad_morh	0.0098	3.0109	D	Q1, Q3
Gaidropsarus		0.01	3	D	Q1
Gaidropsarus mediterraneus	Gai_medi	0.0133	2.8387	D	Q1
Gaidropsarus vulgaris	Gai_vulg	0.0051	3.1481	D	Q1, Q3
Galeorhinus galeus	Gal_gale	0.0038	3.0331	D	Q1, Q3
Gasterosteidae		0.01	3	D	Q1
Gasterosteus aculeatus	Gas_acul	0.01	3	D	Q1, Q3
Glyptocephalus cynoglossus	Gly_cyno	0.0033	3.2048	D	Q1, Q3
Gobiidae		0.01	3	D	Q1, Q3
Gobius		0.01	3	D	Q1
Gobius cobitis	Gob_cobi	0.01	3	D	Q1
Gobius niger	Gob_nige	0.0056	3.3081	D	Q1, Q3
Gymnammodytes semisquamatus	Gym_semi	0.0489	2.0911	D	Q1, Q3
Helicolenus dactylopterus	Hel_dact	0.0104	3.09109	D	Q1, Q3
Hippoglossoides platessoides	Hip_plat	0.0105	2.9029	D	Q1, Q3
Hippoglossus hippoglossus	Hip_hipp	0.0023	3.3796	D	Q1, Q3
Hyperoplus		0.01	3	D	Q1, Q3
Hyperoplus immaculatus	Hyp_imma	0.0056	2.8225	D	Q1, Q3
Hyperoplus lanceolatus	Hyp_lanc	0.0087	2.6262	D	Q1, Q3
Labrus bergylta	Lab_berg	0.0127	3.1048	D	Q1
Labrus mixtus	Lab_mixt	0.0069	3.2084	D	Q1
Lampetra fluviatilis	Lam_fluv	0.01	3	D	Q1, Q3
Lepadogaster		0.01	3	D	Q1
Lepidorhombus whiffiagonis	Lep_whif	0.0058	3.0736	D	Q1, Q3
Leptoclinus maculatus	Lep_macu	0.01	3	D	Q3
Lesueurigobius friesii	Les_frie	0.0641	2.1122	D	Q1
Leucoraja circularis	Leu_circ	0.01	3	D	Q1, Q3
Leucoraja fullonica	Leu_full	0.0033	3.098	D	Q1, Q3

Leucoraja naevus	Leu_naev	0.0036	3.1399	D	Q1, Q3
Limanda limanda	Lim_lima	0.0171	2.8468	D	Q1, Q3
Liparis		0.01	3	D	Q1
Liparis liparis	Lip_lipa	0.01	3	D	Q1, Q3
Liparis montagui	Lip_mont	0.01	3	D	Q1, Q3
Lophiidae		0.01	3	D	Q1
Lophius budegassa	Lop_bude	0.0259	2.8575	D	Q1, Q3
Lophius piscatorius	Lop_pisc	0.0266	2.8614	D	Q1, Q3
Lumpenus lampretaeformis	Lum_lamp	0.0342	1.9847	D	Q1, Q3
Lycenchelys sarsii	Lyc_sars	0.01	3	D	Q3
Lycodes gracilis	Lyc_grac	0.01	3	D	Q3
Lycodes vahlii	Lyc_vahl	0.01	3	D	Q1, Q3
Maurolicus muelleri	Mau_muel	0.1149	1.6065	P	Q1, Q3
Melanogrammus aeglefinus	Mel_aegl	0.0083	3.0473	D	Q1, Q3
Merlangius merlangus	Mer_merl	0.0082	3.0059	D	Q1, Q3
Merluccius merluccius	Mer_merl	0.006	3.0363	D	Q1, Q3
Micrenophrys lilljeborgii	Mic_lill	0.01	3	D	Q1
Microchirus variegatus	Mic_vari	0.0185	2.8546	D	Q1, Q3
Micromesistius poutassou	Mic_pout	0.0047	3.1074	D	Q1, Q3
Microstomus kitt	Mic_kitt	0.0106	3.0419	D	Q1, Q3
Molva dypterygia	Mol_dypt	0.01	3	D	Q1
Molva molva	Mol_molv	0.0036	3.108	D	Q1, Q3
Mugilidae		0.01	3	P	Q1, Q3
Mullus barbatus	Mul_barb	0.01	3	D	Q1, Q3
Mullus surmuletus	Mul_surm	0.0092	3.1048	D	Q1, Q3
Mustelus		0.01	3	D	Q1, Q3
Mustelus asterias	Mus_aste	0.01	3	D	Q1, Q3
Mustelus mustelus	Mus_must	0.01	3	D	Q1, Q3
Myoxocephalus quadricornis	Myo_quad	0.01	3	D	Q1
Myoxocephalus scorpioides	Myo_scor	0.01	3	D	Q1, Q3
Myoxocephalus scorpius	Myo_scor	0.0273	2.8524	D	Q1, Q3
Myxine glutinosa	Myx_glut	0.0167	2.2466	D	Q1, Q3
Nerophis ophidion	Ner_ophi	0.01	3	D	Q1
Osmerus eperlanus	Osm_eper	0.01	3	D	Q1, Q3
Pagellus erythrinus	Pag_eryt	0.01	3	D	Q1
Pegusa lascaris	Peg_lasc	0.008	3.1282	D	Q1
Petromyzon marinus	Pet_mari	3.00E-04	3.4046	D	Q1, Q3
Pholis gunnellus	Pho_gunn	0.0138	2.4873	D	Q1, Q3
Phrynorhombus norvegicus	Phr_norv	0.01	3	D	Q1, Q3
Phycis blennoides	Phy_blen	0.0051	3.1469	D	Q1, Q3
Platichthys flesus	Pla_fles	0.0244	2.7853	D	Q1, Q3
Pleuronectes platessa	Ple_plat	0.0151	2.8876	D	Q1, Q3
Pollachius pollachius	Pol_poll	0.0076	3.0686	D	Q1, Q3
Pollachius virens	Pol_vire	0.0085	3.0242	D	Q1, Q3
Pomatoschistus		0.01	3	D	Q1, Q3
Pomatoschistus microps	Pom_micr	0.01	3	D	Q1
Pomatoschistus minutus	Pom_minu	0.0062	3.173	D	Q1, Q3
Pomatoschistus pictus	Pom_pict	0.0073	3.02	D	Q1
Raja		0.01	3	D	Q1, Q3
Raja brachyura	Raj_brac	0.0027	3.258	D	Q1, Q3

Raja clavata	Raj_clav	0.0045	3.0961	D	Q1, Q3
Raja montagui	Raj_mont	0.0041	3.1152	D	Q1, Q3
Raja undulata	Raj_undu	0.004	3.1346	D	Q1
Rajidae		0.01	3	D	Q1, Q3
Raniceps raninus	Ran_rani	0.0062	3.2667	D	Q1, Q3
Salmo salar	Sal_sala	0.01	3	P	Q3
Salmo trutta	Sal_trut	0.01	3	P	Q1, Q3
Sardina pilchardus	Sar_pilc	0.0053	3.1619	P	Q1, Q3
Scomber scombrus	Sco_scom	0.0014	3.544	P	Q1, Q3
Scophthalmus maximus	Sco_maxi	0.0149	3.0791	D	Q1, Q3
Scophthalmus rhombus	Sco_rhom	0.014	3.0096	D	Q1, Q3
Scyliorhinus canicula	Scy_cani	0.0022	3.1194	D	Q1, Q3
Scyliorhinus stellaris	Scy_stel	0.0045	3.0155	D	Q1, Q3
Sebastes norvegicus	Seb_norv	0.01	3	D	Q1, Q3
Sebastes viviparus	Seb_vivi	0.0115	3.1369	D	Q1, Q3
Sepia officinalis	Sep_offi	0.01	3	D	Q1, Q3
Solea solea	Sol_sole	0.008	3.0499	D	Q1, Q3
Soleidae		0.01	3	D	Q1
Sparidae		0.01	3	D	Q1
Spinachia spinachia	Spi_spin	0.01	3	D	Q1
Spondyliosoma cantharus	Spo_cant	0.0148	3.0044	D	Q1, Q3
Sprattus sprattus	Spr_spra	0.0088	2.9193	P	Q1, Q3
Squalus acanthias	Squ_acan	0.0017	3.208	D	Q1, Q3
Stichaeidae		0.01	3	D	Q1, Q3
Symphodus melops	Sym_melo	0.01	3	D	Q1
Syngnathidae		0.01	3	D	Q1, Q3
Syngnathus		0.01	3	D	Q1
Syngnathus acus	Syn_acus	6.00E-05	3.527	D	Q1, Q3
Syngnathus rostellatus	Syn_rost	1.00E-04	3.414	D	Q1, Q3
Syngnathus typhle	Syn_typh	0.01	3	D	Q1
Taurulus bubalis	Tau_buba	0.0161	3.0785	D	Q1, Q3
Trachinus draco	Tra_drac	0.0087	2.9231	D	Q1, Q3
Trachurus trachurus	Tra_trac	0.0105	2.9622	P	Q1, Q3
Trachyrincus murrayi	Tra_murr	0.01	3	D	Q1
Triglidae		0.01	3	D	Q1, Q3
Trigloporus lastoviza	Tri_last	0.017	2.8685	D	Q1, Q3
Triglops murrayi	Tri_murr	0.01	3	D	Q1, Q3
Trisopterus esmarkii	Tri_esma	0.01	3	D	Q1, Q3
Trisopterus luscus	Tri_lusc	0.0151	2.9459	D	Q1, Q3
Trisopterus minutus	Tri_minu	0.0117	2.9452	D	Q1, Q3
Zeiformes		0.01	3	D	Q1
Zeugopterus punctatus	Zeu_punc	0.0206	3.024	D	Q1, Q3
Zeugopterus regius	Zeu_regi	0.0129	3.2052	D	Q1
Zeus faber	Zeu_fabe	0.0399	2.7536	D	Q1, Q3
Zoarces viviparus	Zoa_vivi	0.0417	2.2532	D	Q1, Q3
Zoarcidae		0.01	3	D	Q3